8th International Symposium on Magnetic Bearing
August 26-28, 2002, Mito, Japan

Reduction of Eddy Current Loss in Small-Sized Active Magnetic Bearing with Solid Cores and Rotor

Ha-Yong Kim
Center for Noise and Vibration Control, KAIST Science Town, Daejeon 305-701, Korea
hykim@novic.kaist.ac.kr

Chong-Won Lee
Center for Noise and Vibration Control, KAIST Science Town, Daejeon 305-701, Korea
cwlee@novic.kaist.ac.kr

ABSTRACT
As the size of rotor with active magnetic bearings (AMBs) gets smaller, lamination of cores and rotor becomes increasingly difficult to effectively reduce the eddy current effect. Thus the accurate modeling of eddy current loss becomes important for the small-sized AMB systems with solid cores and rotor. In this paper, the conventional eddy current loss model is improved based on the eddy current brake concept. It is shown that the eddy current loss in AMBs strongly depends on the arrangement and size of poles. Test results with the hetero- and homo-polar AMBs with non-laminated cores and rotor are compared for verification of analytical findings in relation to the eddy current loss model. The experimental results confirm that the eddy current loss in the small-sized homo-polar AMB with non-laminated cores and rotor can be considerably reduced by optimizing the arrangement and size of poles.

INTRODUCTION
The power losses in AMBs are very important in many applications. In flywheel and aircraft gas turbine applications, major objective is the minimization of the power loss, in order to maximize the operation time of rotor. The power losses have three components: hysteresis loss, eddy current loss and windage loss. To minimize the eddy current loss among these, lamination configuration has been applied to most AMBs. However, as AMBs are employed in a small-sized machine, it is hard to reduce the eddy current loss by lamination using conventional materials.
Matsumura and Hatake [1] suggested an eddy current loss model based on Fourier analysis of the magnetic flux. Based on analytical and experimental results, Allaire, et al. [2][3] proposed a frequency-dependent eddy current loss model, which is a function of the number of poles. They also analyzed the power loss variation with respect to the air gap, bias flux, and number of poles. But, such eddy current models based on the change of magnetic flux are not efficient in investigating the eddy current loss in AMBs, when the arrangement and number of poles are varied [2]. In such cases, use of the eddy current brake model may be more efficient, since the model is based on the movable charge, not the magnetic flux change [4][5].
In this paper, we propose an analytical expression based on the eddy current brake model for the eddy current loss. Utilizing the design factors that are determined through analysis of the eddy current, a homo-polar AMB with solid cores and rotor is constructed for high-speed operation. Run-down test results confirm that the proposed eddy current loss model is effective in optimizing the design of small-sized high-speed AMB systems.

ANALYSIS OF EDDY CURRENTS
When a conducting rod with a constant velocity v moves perpendicular to the rod and also perpendicular to a constant **B** as shown in Fig. 1, the electric field intensity induced in the rod is given by

$$\mathbf{E}' = \mathbf{E} + \mathbf{v} \times \mathbf{B} \tag{1}$$

where **E** and **E**′ are the electric field intensity with respect to the stationary and moving frames, respectively. Then the current due to movable charges generates the motional *emf* (electric motive force) at the rod. However, since the circuit is not complete and thus there can be no current induced in the rod, **E**′ vanishes and **E** in the rod equals to $-\mathbf{v} \times \mathbf{B}$. The movable charges of the conducting rod are subject to the magnetic force $q\mathbf{v} \times \mathbf{B}$

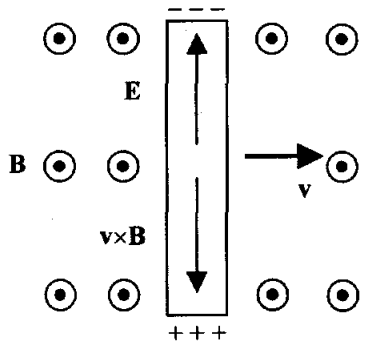

FIGURE 1: A moving conductor at a constant velocity

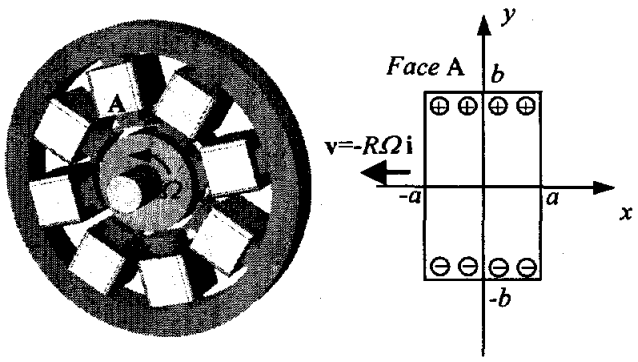

FIGURE 2: Charge density in projected pole face on rotor with constant velocity

that is directed downward along the rod. This leads to a separation of charges: negative charges move upward, whereas positive ones move downward. The separated charges produce an electric field pointing upward that tends to decrease the total force imposed on a given charge in the interior. On the other hand, for the case when there is a current induced in the pole projection area, the electric field intensity becomes $\mathbf{E} \neq -\mathbf{v} \times \mathbf{B}$ [6]. Using the Coulomb's law, the electric field intensity **E** can be derived from a surface charge density $\pm\rho_s = \pm\varepsilon_0 vB$, ε_0 being the permittivity of free space. Figure 2 shows the AMB plane with 8 poles and a projected pole face with constant magnetic field on rotor. Here, a and b are the width and length of the rotor projected pole face, respectively; v, Ω and R are the linear surface velocity, the rotational velocity and the radius of rotor. For one pole AMB, the total electric field intensity E can be represented as

$$\mathbf{E} = E_x\mathbf{i} + E_y\mathbf{j} \tag{2}$$

Here, E_x and E_y are the x and y components of **E**, which can be derived as

$$E_x(x,y) = \frac{vB}{4\pi}\ln\frac{\left[(a-x)^2+(b+y)^2\right]\left[(a+x)^2+(b-y)^2\right]}{\left[(a-x)^2+(b-y)^2\right]\left[(a+x)^2+(b+y)^2\right]} \tag{3}$$

$$E_y(x,y) = -\frac{vB}{2\pi}\left(\tan^{-1}\frac{(a-x)}{(b-y)} + \tan^{-1}\frac{(a-x)}{(b+y)} + \tan^{-1}\frac{(a+x)}{(b-y)} + \tan^{-1}\frac{(a+x)}{(b+y)}\right) \tag{4}$$

For AMB with multi-poles, the neighboring poles will affect the electric field of the pole of interest. According to the arrangement of poles, AMBs are classified into two types: the alternating (NSNSNSNS) and paired (NNSSNNSS) pole configurations. Thus, it is enough to consider two cases for analysis of electric field intensity: arrangements with N-N-S and S-N-S (or, equivalently, S-S-N and N-S-N). The total electric field intensity of the pole of interest can be expressed as, for the alternating pole configuration,

$$E_x = E_x(x,y) - E_x(x+h+2a,y) - E_x(x-h-2a,y) \tag{5}$$
$$E_y = E_y(x,y) - E_y(x+h+2a,y) - E_y(x-h-2a,y) \tag{6}$$

and, for the paired pole configuration,

$$E_x = E_x(x,y) - E_x(x+h+2a,y) + E_x(x-h-2a,y) \tag{7}$$
$$E_y = E_y(x,y) - E_y(x+h+2a,y) + E_y(x-h-2a,y). \tag{8}$$

The total electric field intensity, which is a function of x and y, accounts for both the inside and outside of the projected pole area. The current density is then given as

$$J'_x = \sigma E_x \qquad (everywhere) \tag{9}$$

$$J'_y = \begin{cases} \sigma\left(E_y + vB_z\right) & (inside) \\ \sigma E_y & (outside) \end{cases} \tag{10}$$

Here σ is the conductivity. Since the magnetic flux density, B_z, is zero outside the projection area, the current density inside the pole projection is considered for determination of braking force. The magnetic braking force due to the eddy current is given by

$$\mathbf{F} = \sigma\int \mathbf{J}'\times\mathbf{B}\,d\tau \tag{11}$$

Here, **J'** corresponds to the eddy current density. Since the braking force is generated at all poles simultaneously,

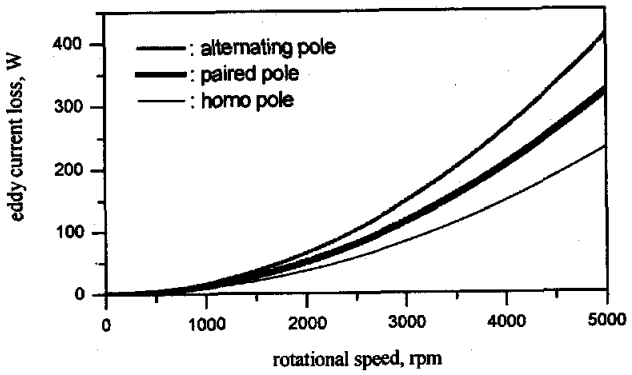

FIGURE 3: Eddy current loss with respect to the arrangement of pole: h=1.8mm, a= 1.8mm, b=6.3mm

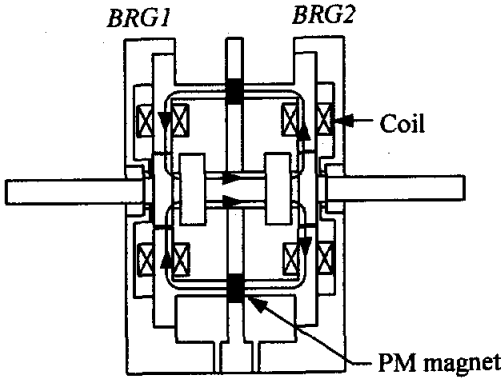

FIGURE 4: Schematic of the proposed homo-polar magnetic bearing

the number of pole, n_p, should be multiplied by the force equation, to yield the total eddy current power loss at AMB, i.e.

$$P_{total} = n_p F v \tag{12}$$

Figure 3 shows the typical eddy current loss calculated for various pole arrangement types. The braking force depends on the pole configuration. For the homo-polar configuration (N-N-N, or S-S-S), the pitch length can be made so small that the eddy current density can be significantly decreased. However, for the alternating pole configuration (S-N-S or N-S-N), the eddy current density is hardly affected by pitch length, because of presence of alternating electric fields in the neighboring projected pole areas. Thus it can be concluded that the AMBs with small pitch and paired poles generate less braking force due to the eddy current than other types.

PROTOTYPE AMB FOR REDUCTION OF EDDY CURRENT POWER LOSS

A homo-polar AMB and a hetero-polar AMB were built

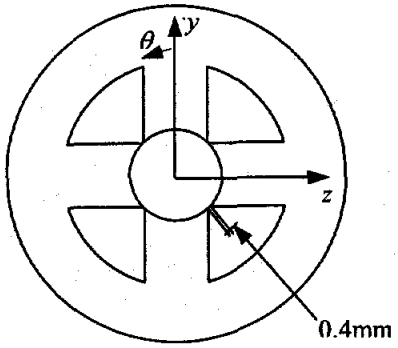

FIGURE 5: Coordinate system in stator

TABLE 1: Design parameters

parameter	*value*	*parameter*	*value*
Area of pole	115mm^2	*Br of PM*	1.18T
Air gap	0.2mm	*Hc of PM*	867kA/m
Rotor diameter	20mm	*Coil turns*	160
Bearing span	58mm	*Rotor mass*	264g
PM length	4mm	K_y[N/m]	7.46×10^4
PM area	144mm^2	K_i[N/A]	38.6 A

with non-laminated cores and rotor in order to effectively investigate the eddy current loss associated with pole configuration. To reduce the eddy current loss, the number of poles should be kept as small as possible. At least, four poles are normally required for linear control of AMB. The pitch length is determined so that the control flux leakage is minimized in the neighboring poles. The schematics of the proposed homo-polar AMB are shown in Figs. 4 and 5, and its design parameters are listed in Table 1. The pitch length of stator is 0.4mm and, for the control flux of 4.62×10^{-5}Wb, the leakage flux is calculated to be 1.76×10^{-9}Wb, which is negligibly small. As the proposed homo-polar AMB with pitch length of 0.4 mm can be considered to be almost slot-less, the magnetic flux in the y direction is approximated as

$$\phi = \phi_{pg} + \phi_c \quad \left(-\frac{\pi}{4} \le \theta \le \frac{\pi}{4}\right) \tag{13}$$

$$\phi = \phi_{pg} - \phi_c \quad \left(\frac{3\pi}{4} \le \theta \le \frac{5\pi}{4}\right) \tag{14}$$

The magnetic force can be linearized with respect to the equilibrium using the relation between the bias flux ϕ_{pg} and the control flux ϕ_c, i.e.

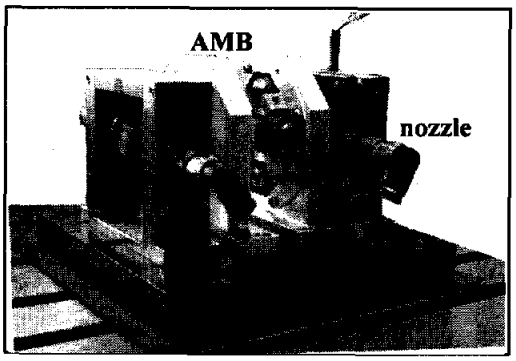

FIGURE 6: Experimental setup of AMB system

$$F(y,i)=\frac{1}{\mu_0 A_g}\left\{\left(\frac{H_m l_m}{R_p}+\frac{\mu_0 A_g N i}{2g_{oc}}\right)^2-\left(\frac{H_m l_m}{R_p}-\frac{\mu_0 A_g N i}{2g_{oc}}\right)^2\right\}$$
$$=K_{y_1}y_1+K_{y_2}y_2+K_{i_{y1}}i_{y_1} \tag{15}$$

And the magnetic permeance, P_p is obtained, from the position of rotor, as

$$P_p=\frac{1}{R_p}=\frac{\int\frac{\mu_0 Rw}{g_{op}-y_1\cos\theta-z_1\sin\theta}d\theta\int\frac{\mu_0 Rw}{g_{op}-y_2\cos\theta-z_2\sin\theta}d\theta}{\int\frac{\mu_0 Rw}{g_{op}-y_1\cos\theta-z_1\sin\theta}d\theta+\int\frac{\mu_0 Rw}{g_{op}-y_2\cos\theta-z_2\sin\theta}d\theta} \tag{16}$$

Note that the magnetic permeance, instead of the magnetic reluctance, is more convenient for AMB analysis. Permanent magnet flux, which forms the common bias flux in a pair of AMBs, passes through both the bearing plane and shaft as shown in Fig. 4, resulting in permeance coupling in each AMBs. It requires a centralized control for the AMB system due to the presence of the heavily coupled terms in the equation of motion.

EXPERIMENTS

Figure 6 shows the experimental setup, which is equipped with two nozzles and an impeller at each bearing plane, in order to generate the rotational force using the compressed air of maximum pressure equal to 3×10^5 Pa. Tests for braking force measurement were carried out with the hetero- and homo-polar magnetic bearings. Both AMBs were built with the solid cores and rotor. Figures 7(a) and (b) compare the run-down test performance and the resulting power loss, respectively, for three different bearings: ball bearing, hetero-polar AMB and homo-polar AMB. The braking force due to eddy current, which drastically increases as the rotational speed increases, for the hetero-polar AMB limited the test rotational speed to 5,000 rpm. Note that the power

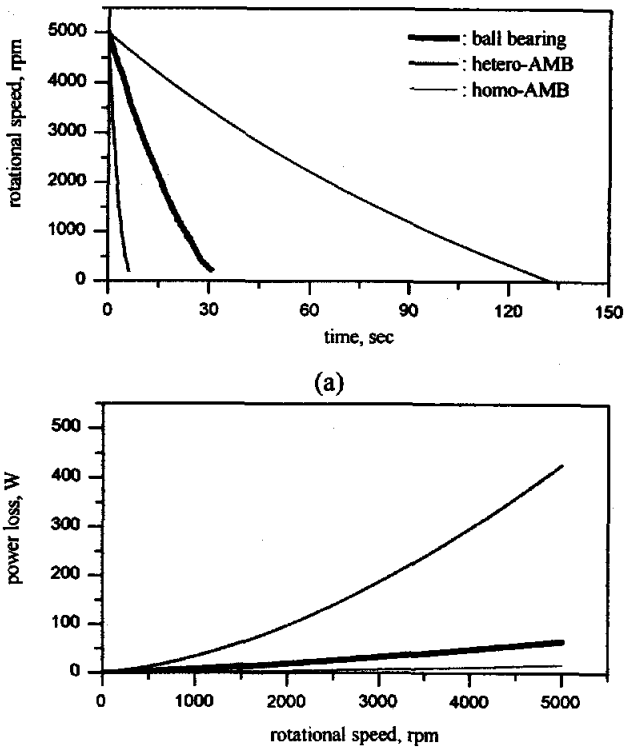

FIGURE 7: (a) Run-down test performance and (b) power loss for ball bearing, hetero-polar AMB and homo-polar AMB.

loss of the hetero-polar AMB was 426W at 5000 rpm, about 20 times as much as that of the homo-polar AMB. As the power loss measured through the run-down test is composed of the hysteresis, eddy current and windage losses, the eddy current loss was estimated from the model given by [2][3]

$$P=C_h\omega+C_e\omega^2+C_{w\_ex}(\omega) \tag{17}$$

Here, P is the total power loss; C_h and C_e are the coefficient of the hysteresis and the eddy current loss, respectively; ω is the rotational speed; $C_{w\_ex}(\omega)$ is the experimentally determined windage loss. Figure 8 indicates that the measured and computed eddy current losses with the rotational speed varied for the hetero-polar AMB are in good agreement with fair accuracy. Figure 9 shows the eddy current loss for the hetero-polar AMB, when the area of pole face is kept identical to the area of pitch, i.e. $A_{pitch}=A_{face}$=25.7mm^2. Note that the eddy current loss is nearly independent of the arrangement of poles, falling within 10% error bounds. Although the computed values are not in good agreement with the measured values [1], the tendency remains the same. Figure 10 shows the whirl orbit was

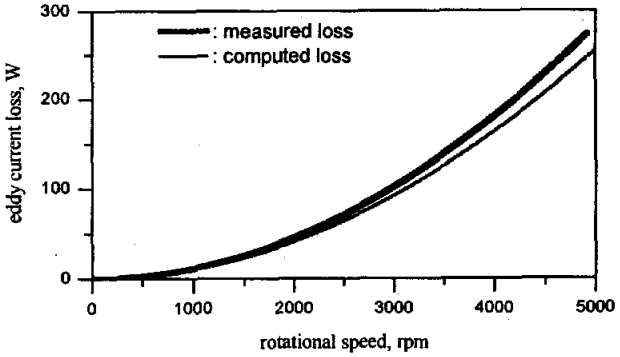

FIGURE 8: Measured and computed eddy current losses

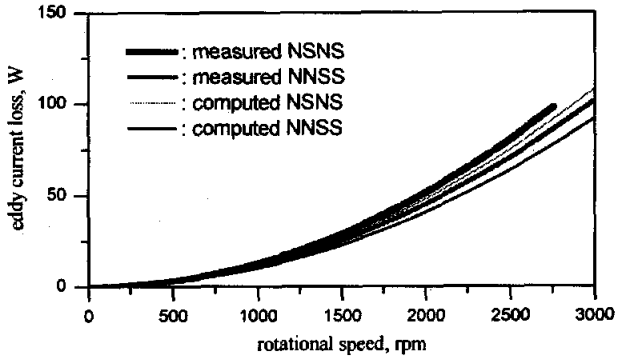

FIGURE 9: Effect of pole configuration on power loss

kept within 15μm for the homo-polar AMB running at 40,000 rpm. Considering the nominal air gap of 200μm (the clearance of touch-down bearing is 100μm) and the high operating speed of 40,000 rpm, the performance of the homo-polar AMB was as excellent as expected from analysis.

CONCLUSIONS

We proposed the analytical expressions for the eddy current loss based on the eddy current brake concept. To obtain the electric field intensity, the concept of the movable charge and Coulomb's law was applied. Since AMBs have multi-poles unlike the single-pole eddy current brake, the electric field intensity depends on the arrangement of poles and the size of pitch and pole. It is concluded that reduction in the pitch length and the current circulation on rotor by employing homo-polar configuration can minimize the eddy current in the pole projection areas. To experimentally verify the analytical findings, a homo-polar AMB was designed and built with solid cores and rotor. Run-down tests were performed to compare the homo-polar AMB with the hetero-polar AMB in eddy current loss.

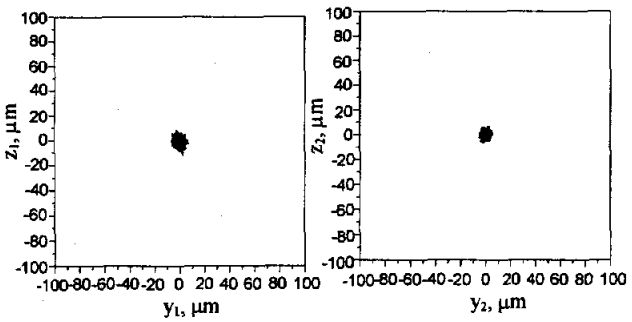

FIGURE 10: Whirl orbit: homo-polar AMB at 40,000rpm

REFERENCES

1. Matsumura, F., and Hatake, K., Relation between Magnetic Pole Arrangement and Magnetic Loss in Magnetic Bearing, Proc. of 3rd ISMB, Alenxadria, Virginia, USA, 1992, pp.274-283.
2. Kasarda, M. E. F., and Allaire, P. E., Comparison of Predicted and Measured Rotor Losses in Planar Radial Magnetic Bearings, ASME Journal of Tribology, vol.40, no.2, 1997, pp.219-226.
3. Allaire, P. E., et al., Rotor Power Losses in Planar Radial Magnetic Bearings-Effects of Number of Stator Poles, Air Gap Thickness, and Magnetic Flux Density, ASME Journal of Engineering for Gas Turbines and Power, vol.121, 1999, pp.691-696.
4. Heald, M. A., Magnetic Braking: Improved Theory, American Journal of Physics, vol.56, no.6, 1988, pp.521-522.
5. Lee, K., and Park, K., Eddy Currents Modeling with the Consideration of the Magnetic Reynolds Number, Proc. of ISIE, Busan, Korea, 2001, pp.678-683.
6. Wangsness, R. K., *Electromagnetic field*, John Wiley & Sons Inc, 2nd ed., 1986.